ISSN 1063-7834, Physics of the Solid State, 2021, Vol. 63, No. 9, pp. 1530–1534. © Pleiades Publishing, Ltd., 2021.
Russian Text © The Author(s), 2021, published in Fizika Tverdogo Tela, 2021, Vol. 63, No. 9, pp. 1367–1371.

LOW-DIMENSIONAL SYSTEMS

Why the Magnetite–Gold Core–Shell Nanoparticles Are Not Quite Good and How to Improve Them

A. E. Sokolov[a, b], O. S. Ivanova[a, b], A. S. Fedorov[a, b, c], E. A. Kovaleva[c], M. A. Vysotin[a, b], C.-R. Lin[d], and S. G. Ovchinnikov[a, b, *]

[a] *Kirensky Institute of Physics, Krasnoyarsk Scientific Center, Siberian Branch, Russian Academy of Sciences, Krasnoyarsk, 660036 Russia*

[b] *Siberian Federal University, Krasnoyarsk, 660041 Russia*

[c] *Tomsk State University, Tomsk, 634050 Russia*

[d] *National Pingtung University, Pingtung City, Pingtung County, 90003 Taiwan*

**e-mail: sgo@iph.krasn.ru*

Received April 9, 2021; revised April 9, 2021; accepted April 19, 2021

Abstract—The nature of the formation of a chemical bond at the magnetite–gold interface has been studied. The geometric structure and the electronic and magnetic properties of plane layers consisting of magnetite Fe_3O_4 and gold have been investigated using the DFT-GGA calculation. It has been found that the specific energy and the wetting parameter of the magnetite–gold interface are negative, which leads to the island growth of small Au particles on the Fe_3O_4 surface. The role of an intermediate thin titanium layer between magnetite and gold has been discussed. The specific energy and wetting parameter of the magnetite–titanium (for thin Ti layers) and magnetite–titanium–gold interfaces are positive. It has been suggested that an intermediate thin titanium layer at the interface between the magnetite nanoparticle surface and the gold layer will make it possible to obtain magnetite nanoparticles with a continuous gold coating.

Keywords: core–shell magnetic nanoparticles, magnetite–gold interface, magnetite–titanium–gold trilayer

DOI: 10.1134/S1063783421090365

1. INTRODUCTION

In recent years, the possibility of using magnetic nanoparticles in biomedicine for magnetic separation, targeted drug delivery, magnetic hyperthermia, magnetomechanical therapy, improving the MRI contrast, etc. has been intensively studied [1–8]. Meanwhile, the use of magnetic nanoparticles is complicated by their high aggregation and rapid biodegradation at the interaction with biological systems; therefore, magnetic nanoparticles in their pure form are rarely used in therapy. As a rule, they are encapsulated or placed in bioinert matrices from various organic compounds or polymers, including natural ones, in order to reduce the possible toxic effect of the magnetic phase, increase its physicochemical stability, and ensure immobilization on the surface of such capsules or drug matrices [9].

Much attention has recently been paid to the fabrication of core–shell nanostructures, e.g., magnetic iron oxides coated with a noble metal (gold, platinum, silver, or palladium) shell [10–16]. The gold shell provides additional functionality, in particular, for local heating of the metallic layer by external radiation. In addition, such a shell reduces the toxic effect of magnetic nanoparticles on the body. Obtaining of the core–shell nanoparticles was evidenced by schemes [17], electron microscopy data indicating an increase in the nanoparticle size in the course of a chemical reaction [18–20], or X-ray diffraction data showing the dominance of the crystalline gold peaks with increasing thickness of the surface gold layer [21]. On closer analysis, some authors concluded that there is not a continuous coating of magnetite nanoparticles with gold, but rather "decoration" of a coarser nanoparticle with small islands [16, 22–24]. A similar situation is observed during the synthesis of core–shell nanoparticles with silver as a coating. In [23], we also reported the decoration of magnetite nanoparticles with silver during the synthesis of core–shell nanoparticles. Examples of decorated structures are shown in Figs. 1, 2.

In this study, we try to understand the reason for the island growth of small gold nanoparticles on the magnetite surface and clarify if this is related to the fundamental features of the chemical bond formation in such systems. Therefore, we investigate features of the formation of a chemical bond between the magnetite and gold layers using the density functional theory (DFT).

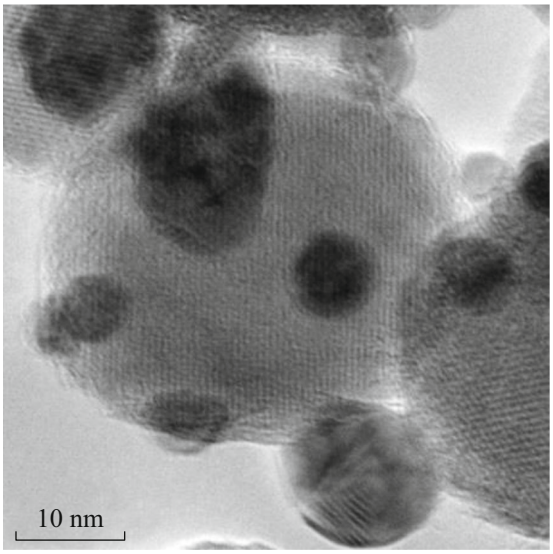

Fig. 1. Decorated Fe_3O_4@Ag nanoparticles.

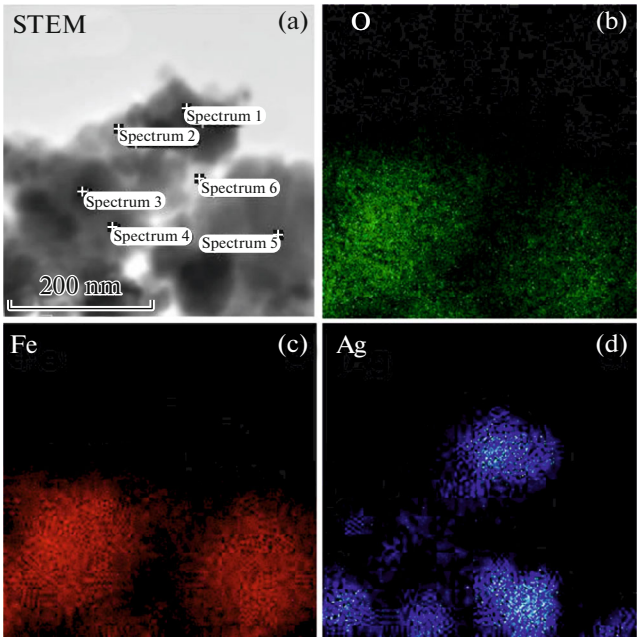

Fig. 2. Electron microscopy image and EDS distribution of elements on the Fe_3O_4@Ag nanoparticles. (For the detailed characterization of the nanoparticles, see our study [23].)

2. CALCULATION TECHNIQUE

Instead of curved surfaces of nanoparticles, we investigated a planar structure consisting of thin Fe_3O_4 and Au layers (slabs). The calculation was made in the spin-polarized version of the DTF in the generalized gradient approximation of Perdew–Burke–Ernzerhof (GGA-PBE) for the exchange correlation potential [25, 26] within the VASP 5.4 package [27, 28]. The interaction between slabs was described with allowance for the Grimme correction [29]. To take into account the correlation effects, we used the LDA + U correction in the form proposed in [30] with a parameter of $U = 4.0$ eV for Fe atoms. The calculation of the total energy of the structure with the geometry optimization was carried out until the residual forces acting on the atoms became weaker than 0.05 eV/Å. In all the calculations, the energy cutoff parameter was 500 eV.

Since the effect of temperature on the lattice parameters is minor and, under standard conditions ($T \sim 300$ K), the interatomic distances change by no more than 1% of the values at $T = 0$, because the average linear expansion coefficients of solids are $\sim 10^{-5}$ K^{-1} in order of magnitude, we performed the quantum chemical calculations at $T = 0$.

First, we calculated the bulk structures of gold and magnetite, for which the obtained lattice parameters are in good agreement with the experimental data. Then, the Fe_3O_4(111) and Au(111) surfaces were build (Fig. 3), as in [31, 32], where the optimal parameters of the magnetite surface were calculated. A vacuum interval of 10 Å between the slabs eliminated the artificial interaction due to the periodic boundary conditions in the direction perpendicular to the interface. According to the Monkhorst–Pack procedure [33], the first Brillouin zone was divided into sets of k points $6 \times 6 \times 6$ and $12 \times 12 \times 12$ for the bulk materials and $6 \times 6 \times 1$ for all the slabs and interfaces [34].

Specific surface energy E_{surf} of an individual Fe_3O_4 and Au slab was calculated by the formula

$$E_{surf} = \frac{E_{slab} - E_{bulk} N_{slab}/N_{bulk}}{2A}, \quad (1)$$

where E_{bulk} and E_{slab} are the total energy of the bulk sample and the slab with number of atoms N_{bulk} and N_{slab}, respectively, and A is the slab surface area. The magnetite layer thickness was specified to be 12 monolayers and the gold layer thickness ranged from 1 to 9 monolayers. The surface energies obtained at different numbers of gold monolayers are given in Table 1. The data obtained allow us to conclude that 5 monolayers of gold are sufficient to reliably calculate specific surface energy E_{surf}.

Knowing the energies of individual slabs, the total energy of the magnetite–gold hybrid structure, and the specific surface energy, we can find the specific energy of the interface between layers 1 and 2 ($E_{int1,2}$)

$$AE_{int1,2} = \sum_{i=1,2} (E_{slab\,i} - AE_{surf\,i}) - E_{hybrid1,2}. \quad (2)$$

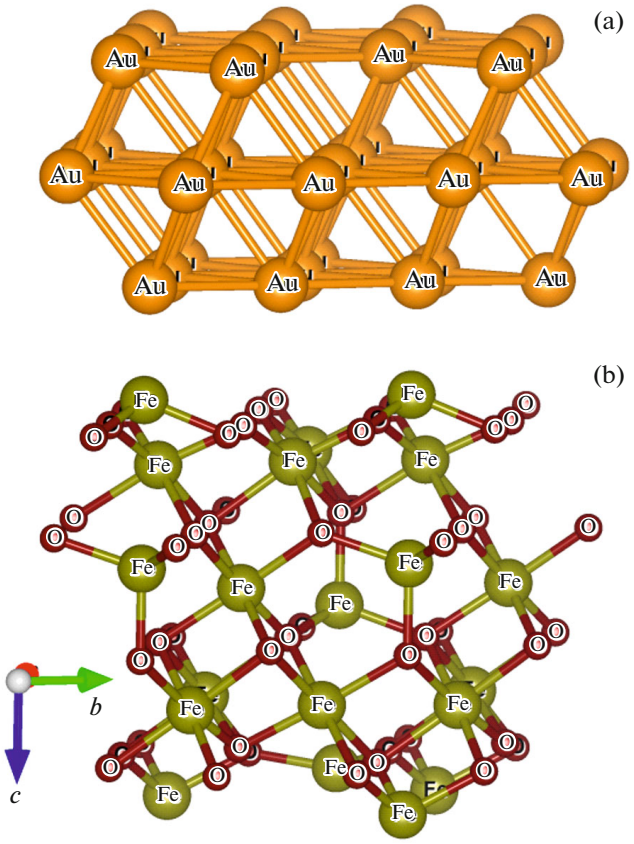

Fig. 3. (a) Magnetite and (b) gold layer structures used in the calculation. Iron atoms are colored in green; oxygen atoms, in red; and gold atoms, in orange. (See the colored figure in the electronic Journal.)

Wetting parameter S, which reflects the total energy variation during the distribution of a liquid gold droplet over the magnetite substrate surface is determined by the formula

$$S_{1,2} = \frac{E_{\text{slab1}} + E_{\text{bulk2}}N_{\text{slab2}}/N_{\text{bulk2}} - E_{\text{hybrid1,2}}}{A}, \quad (3)$$

where $S_{1,2}$ is the parameter of wetting of substrate 1 (magnetite) with droplet 2 (gold).

Table 1. Surface energies of magnetite and gold slabs at different numbers of gold layers on magnetite

Slab	N_{layers}	E_{surf}, J/m^2
Fe_3O_4	12	1.13
Au	1	1.00
Au	3	1.41
Au	5	1.40
Au	9	1.43

3. RESULTS

The obtained interface energies and wetting parameters for the magnetite–gold structure at different numbers (from 1 to 9) of atomic layers of gold are given in Table 2. It can be seen that these parameters are negative at any gold thickness. Thus, the homogeneous Fe_3O_4/Au interface is unstable, which explains the island growth of small gold particles on the surface of a coarse magnetite particle. It was shown in [35] that, in the opposite case, during deposition of magnetite onto a coarse (200 nm) gold nanoparticle, small magnetite islands are also formed. In addition, Table 2 shows that gold negligibly affects the magnetization of Fe_3O_4@Au particles.

To stabilize the Fe_3O_4/Au interface, we propose to introduce an additional thin layer that can form a stable interface with both magnetite and gold. Such properties are typical, for example, of a titanium layer. The interface energies and wetting parameters calculated by formulas (1)–(3) for Fe_3O_4/Ti and Ti/Au turned out to be positive. Figure 4 shows the change in the geometry of the magnetite layer contacting with titanium. Oxygen atoms hidden under the magnetite surface (Fig. 3) emerge to the surface when an intermediate titanium layer is introduced (Fig. 4). This surface reconstruction ensures the stability of the homogeneous Fe_3O_4/Ti interface.

During deposition of gold, the Fe_3O_4/Ti interface acts as a new complex substrate; therefore, its parameter of wetting with Au is calculated using modified formula (3)

$$S_{2,3} = \frac{E_{\text{hybrid1,2}} + E_{\text{bulk3}}N_{\text{slab3}}/N_{\text{bulk3}} - E_{\text{hybrid1,2,3}}}{A}, \quad (4)$$

where $S_{2,3}$ is the parameter of wetting of substrate 1 (magnetite) with already deposited layer 2 (titanium) by droplet 3 (gold). The specific interface energy, wetting parameter, shortest Fe–Ti and Ti–Au distances, and magnetization per cell (4 formula units) of the magnetite–titanium–gold structure with different numbers of gold monolayers are given in Table 3. Our calculations for 5 and 9 Ti monolayers yielded negative wetting parameters of –0.19 and –0.61 J/m^2, respec-

Table 2. Specific interface energy, wetting parameter, shortest distance between Fe and Au atoms, and magnetization per cell (4 formula units) of the magnetite–gold slab with different numbers of gold monolayers

Interface	$E_{\text{int1,2}}$, J/m^2	$S_{1,2}$, J/m^2	$d_{\text{Fe–Au}}$, Å	Magnetization, μ_B
Fe_3O_4/1Au	–0.92	–0.70	2.72	18.50
Fe_3O_4/3Au	–1.32	–1.49	2.78	18.61
Fe_3O_4/5Au	–1.40	–1.54	2.77	18.41
Fe_3O_4/9Au	–1.47	–1.63	2.59	18.86

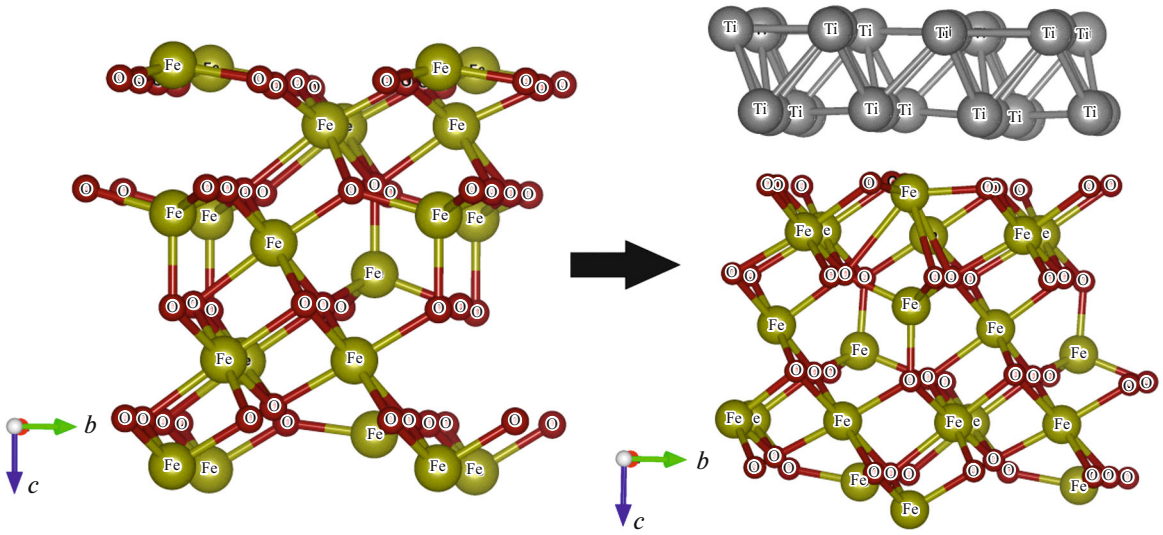

Fig. 4. Modification of the magnetite surface upon introduction of an intermediate titanium layer. Iron atoms are colored in green; oxygen atoms, in red; and titanium atoms, in grey. (See the colored figure in the electronic Journal.)

tively; therefore, we can state that the intermediate titanium layer should really be of atomic thickness.

In addition, we examined the electronic and magnetic properties of all the investigated layered structures. The analysis of the partial densities of electronic states allowed us to establish that the magnetite–titanium–gold layers are conductive due to the gold layer; no significant changes in the magnetic moments occur on the iron atoms.

4. CONCLUSIONS

In this study, we investigated the nature of the formation of a chemical bond at the magnetite–gold interface and found that an intermediate titanium layer can stabilize the structure of nanoparticles with a magnetic core–gold shell structure. Using the DFT-GGA calculations, the geometric structure and the electronic and magnetic properties of the plane layers consisting of magnetite Fe_3O_4, titanium, and gold were investigated.

The total and specific surface energies of the isolated magnetite, titanium, and gold plates, as well as the bi- and trilayers formed via their surface contact, the specific energies of interfaces and wetting parameters were calculated for the magnetite–gold, magnetite–titanium, and titanium–gold interfaces. It was established that the specific energy and wetting parameter of the magnetite–gold interface are negative, while these values for the magnetite–titanium (for thin Ti layers) and magnetite–titanium–gold interface are positive. This allows us to believe that the intermediate thin titanium layer at the interface between the magnetite nanoparticle surface and the gold layer stabilizes this trilayer and will make it possible to obtain magnetite nanoparticles with a continuous gold coating.

The electronic and magnetic properties of all the investigated layered structures were studied. Analyzing the partial density of electronic states, we found that the magnetite–titanium–gold layers are conductive due to the gold layer; no significant changes in the magnetic moments on iron atoms occur. In general, the calculation showed that the titanium buffer layer stabilizes the magnetite–titanium–gold plates, which

Table 3. Specific interface energy, wetting parameter, shortest Fe–Ti and Ti–Au distances, and magnetization of the magnetite–titanium–gold slab with different numbers of gold monolayers

Interface	E_{int}, J/m^2	S, J/m^2	d_{Fe-Ti}, Å	d_{Ti-Au}, Å	Magnetization, μ_B
Fe_3O_4/2 Ti	1.23	0.13	2.73		17.62
Fe_3O_4/2 Ti/1Au	0.75	2.08	2.72	2.73	17.92
Fe_3O_4/2 Ti/3Au	0.88	1.82	2.73	2.74	18.00
Fe_3O_4/2 Ti/5Au	0.82	1.79	2.75	2.74	17.87
Fe_3O_4/2 Ti/9Au	0.80	1.74	2.73	2.73	17.91

should facilitate the synthesis of gold-coated magnetic magnetite nanoparticles.

Based on the reported investigations, we can give a qualitative recipe for which layer and when can be used to solve the problem of wettability. In this case, gold does not form an oxide; therefore, there is no continuous coating of iron oxide with a gold shell. Titanium, on the contrary, forms an oxide and therefore easily creates a monoatomic shell. It can be said that an oxidizable layer should always be deposited onto the oxide surface first and, then, a gold layer can be added, although the options with a non-oxidizable element having good adhesion to the surface of another oxide are also possible.

FUNDING

This study was supported by the Russian Foundation for Basic Research, project no. 19-52-52002, and the Ministry of Science and Technology of Taiwan, projects MOST nos. 109-2112-M-153-003 and 108-2923-M-153-001-MY3.

CONFLICT OF INTEREST

The authors declare that they have no conflicts of interest.

REFERENCES

1. V. N. Nikiforov, Izv. Akad. Inzh. Nauk im. A. M. Prokhorova, No. 1, 23 (2013).
2. A. Doaga, A. M. Cojocariu, C. P. Constantin, R. Hempelmann, and O. F. Caltun, AIP Conf. Proc. **1564**, 123 (2013).
3. N. Tran and T. J. Webster, J. Mater. Chem. **20**, 8760 (2010).
4. V. F. Cardoso, A. Francesko, C. Ribeiro, M. Bañobre-López, P. Martins, and S. Lanceros-Mendez, Adv. Healthcare Mater. **7**, 1700845 (2018).
5. M. Mahdavi, M. B. Ahmad, M. J. Haron, F. Namvar, B. Nadi, and M. Z. Ab Rahman, J. Amin. Mol. **18**, 7533 (2013).
6. J. Gao, H. Gu, and B. Xu, Acc. Chem. Res. **42**, 1097 (2009).
7. C. Sun, J. S. H. Lee, and M. Zhang, Adv. Drug Deliv. Rev. **60**, 1252 (2008).
8. P. Tartaj, M. Del Puerto Morales, S. Veintemillas-Verdaguer, T. González-Carreño, and C. J. Serna, J. Phys. D **36**, R182 (2003).
9. K. Chatterjee, S. Sarkar, K. Jagajjanani Rao, and S. Paria, Adv. Colloid Interface Sci. **209**, 8 (2014).
10. S. Laurent, D. Forge, M. Port, A. Roch, C. Robic, L. vander Elst, and R. N. Muller, Chem. Rev. **108**, 2064 (2008).
11. S. Venkateswarlu, B. Natesh Kumar, B. Prathima, K. Anitha, and N. V. V. Jyothi, Phys. B (Amsterdam, Neth.) **457**, 30 (2015).
12. Z. Wang, B. Shen, Z. Aihua, and N. He, Chem. Eng. J. **113**, 27 (2005).
13. A. Bachhuka, S. N. Christo, A. Cavallaro, K. R. Diener, A. Mierczynska, L. E. Smith, R. Marian, J. Manavis, J. D. Hayball, and K. Vasilev, Adv. Colloid Interface Sci **457**, 9 (2015).
14. P. D. Rudakovskaya, E. K. Beloglazkina, A. G. Mazhuga, N. L. Klyachko, A. V. Kabanov, and N. V. Zyk, Mosc. Univ. Chem. Bull. **70**, 149 (2015).
15. A. Yu. Solov'eva, Yu. V. Ioni, A. O. Baskakov, S. S. Starchikov, A. S. Avilov, I. S. Lyubutin, and S. P. Gubin, Russ. J. Inorg. Chem. **62**, 711 (2017).
16. M. V. Efremova, Yu. A. Nalench, E. Myrovali, A. S. Garanina, I. S. Grebennikov, P. K. Gifer, M. A. Abakumov, M. Spasova, M. Angelakeris, A. G. Savchenko, M. Farle, N. Klyachko, A. Majouga, and U. Wiedwald, Beilstein J. Nanotechnol. **9**, 2684 (2018).
17. A. M. El-Toni, M. A. Habila, J. P. Labis, Z. A. Alothman, M. Alhoshan, A. A. Elzatahry, and F. Zhang, Nanoscale **8**, 2510 (2016).
18. L. Wang, J. Luo, Q. Fan, M. Suzuki, I. S. Suzuki, M. H. Engelhard, Yu. Lin, N. Kim, J. Q. Wang, and Chuan-Jian Zhong, J. Phys. Chem. B **109**, 21593 (2005).
19. H. Y. Park, M. J. Schadt, L. Wang, I-Im. S. Lim, P. N. Njoki, S. H. Kim, M. Y. Jang, J. Luo, and C. J. Zhong, Langmuir **23**, 9050 (2007).
20. U. Tamer, Y. Gundogdu, I. H. Boyaci, and K. Pekmez, J. Nanopart. Res. **12**, 1187 (2010).
21. Z. Xu, Y. Hou, and S. Sun, J. Am. Chem. Soc. **129**, 8698 (2007).
22. H. Maleki, A. Simchi, M. Imani, and B. F. O. Costa, J. Magn. Magn. Mater. **324**, 3997 (2012).
23. D. A. Petrov, C.-R. Lin, R. D. Ivantsov, S. G. Ovchinnikov, S. M. Zharkov, G. Y. Yurkin, D. A. Velikanov, Y. V. Knyazev, M. S. Molokeev, Y.-T. Tseng, E.-S. Lin, I. S. Edelman, A. O. Baskakov, S. S. Starchikov, and I. S. Lyubutin, Nanotechnology **31**, 395703 (2020).
24. S. V. Saikova, T. V. Trofimova, A. Yu. Pavlikov, D. V. Karpov, D. I. Chistyakov, and Yu. L. Mikhlin, Russ. Chem. Bull. **69**, 1284 (2020).
25. P. E. Blöchl, Phys. Rev. B **50**, 17953 (1994).
26. G. Kresse and D. Joubert, Phys. Rev. B **59**, 1758 (1999).
27. G. Kresse and J. Furthmuller, Comput. Mater. Sci. **6**, 15 (1996).
28. G. Kresse and J. Furthmuller, Phys. Rev. B **54**, 11169 (1996).
29. S. Grimme, J. Antony, S. Ehrlich, and H. Krieg, J. Chem. Phys. **132**, 154104 (2010).
30. S. Dudarev and G. Botton, Phys. Rev. B **57**, 1505 (1998).
31. J. Noh, O. I. Osman, S. G. Aziz, P. Winget, and J. L. Bredas, Chem. Mater. **27**, 5856 (2015).
32. A. Kiejna and T. Pabisiak, Surf. Sci. **679**, 225 (2019).
33. H. J. Monkhorst and J. D. Pack, Phys. Rev. B **13**, 5188 (1976).
34. A. S. Fedorov, E. A. Kovaleva, A. E. Sokolov, M. A. Vysotin, C. R. Lin, and S. G. Ovchinniko, Mater. Chem. Phys. (2021, in press).
35. M. Torras, A. Gordillo, and A. Roig, Rev. Soc. Catalana Quim. **17**, 107 (2018).

Translated by E. Bondareva